International Environmental Modelling and Software Society (iEMSs)
2012 International Congress on Environmental Modelling and Software
Managing Resources of a Limited Planet, Sixth Biennial Meeting, Leipzig, Germany
R. Seppelt, A.A. Voinov, S. Lange, D. Bankamp (Eds.)
http://www.iemss.org/society/index.php/iemss-2012-proceedings

Application of CFD methods to the upgrading of a contact tank

C. Gualtieri
Hydraulic, Geotechnical and Environmental Engineering Department (DIGA), University of Napoli "Federico II". Italy. carlo.gualtieri@unina.it

Abstract: The paper presents the results of a Computational Fluid Dynamics (CFD) study undertaken to upgrading the hydraulic efficiency of the contact tank of the wastewater treatment plant of Nola-Marigliano, near Napoli. First numerical simulations were performed to compare the hydraulic performances of two existing operating schemes (A and B). The results pointed out the presence of recirculation areas near the baffles and the corners of the tank. Second some different changes were proposed for scheme A, which has shown the best performances, to reduce dead-zones inside the tank. Hence, further numerical simulations pointed out that the introduction of a grid inside the internal walls of the tank allowed to improve its hydraulic performance. Overall, the study demonstrated that CFD methods could be applied to improve the hydraulic performances of existing contact tanks.

***Keywords**:* environmental hydraulics; turbulence, contact tank, numerical simulations, k-ε model; residence time distribution.

1 INTRODUCTION

Disinfection is usually applied in both drinking water and wastewater treatment systems to inactivate micro-organisms, some of which may be pathogenic, preventing transmission of waterborne diseases. Chlorination is the most common disinfection method currently used. This method involves addition of chlorine gas or salts to an aqueous stream moving in a contact tank, which should be designed to achieve the objective to bring as much water in contact with chlorine for as long as possible to obtain a certain level of disinfection. Typically disinfection systems are designed to provide efficient mixing of chlorine solution with raw water for a contact time of at least 30 minutes, with the concentration of free chlorine in the tank effluent between 0.1 and 0.2 mg/L [Gyurek and Finch 1998]. Effective design of chlorine disinfection processes must integrate four major elements [Greene 2002]:

- chlorine and source water chemistry, since the process is affected by both physical and biological characteristics of water, such as suspended solids, temperature, pH, oxidisable substances;
- chlorine decay kinetics, since the loss of chlorine is characterized by an initial rapid loss period known as immediate demand, followed by a slow decay period. The first one could be expressed as:

  $$Cl_{id} = Cl_{in} - Cl_0 \quad (1)$$

  where Cl_{id}, Cl_{in} and Cl_0 are immediate chlorine demand, applied chlorine dose and total initial chlorine residual. The slow decay process is typically modeled with a first-order kinetics;
- microbial inactivation kinetics, which is commonly expressed using a first-order rate (Chick-Watson model). Actually, disinfection systems rarely display first-order kinetics, so different models have been proposed, such as Hom kinetic model, multiple target and series-event models [Gyurek and Finch 1998];

- chlorine contact tank hydraulics, which is the focus of this paper.

As previously outlined, the main objective of the chlorine contact tank is to provide adequate residence time for both the micro-organism and the disinfectant to achieve the desired degree of microbial inactivation. Achieving proper disinfection is generally quantified by the $C \times T$ rule, if C is the minimum disinfectant residual measured at the tank outflow and T is the minimum contact time. The product $C \times T$ must exceed a value that depends on the type of disinfectant used, pH and temperature, as specified in regulatory documents, to obtain a defined level of inactivation for specified micro-organism, based on standardized inactivation rate estimates. The $C \times T$ rule often requires the use of T_{10} as representative of the hydraulic residence time. T_{10} is the residence time of earliest 10% of micro-organism to travel through the tank, as determined from a tracer Residence Time Distribution (RTD). In other words, T_{10} is the RTD tenth percentile. In real contact tanks T_{10} is shorter than the mean hydraulic residence time τ, which is calculated by dividing the tank volume by the water flow rate. Thus, one way to meet the disinfection criteria could be by increasing the chlorine dosage, but this also increases operational costs and may induce high concentrations of dangerous disinfection by-products (DBPS) [Hannoun et al. 1998]. Hence, the best way to optimize disinfection effectiveness is by increasing T_{10} value and by reducing the required disinfectant dosage. To achieve this goal the tank could be enlarged, resulting in additional storage volume, with higher construction and maintenance costs. A more cost-effective way to increase T_{10} is to maximize the uniformity of flow patterns. The maximum T_{10} is equal to τ, if all the water parcels remain for the same time inside the tank, i.e. plug-flow conditions. Thus, and also because most chemical reactions are more effectively completed in a plug-flow reactor [Wang et al. 2003], chlorine contact tanks are typically designed to approach plug-flow conditions. However, real contact tanks cannot achieve these conditions because of velocity gradients caused by flow disturbances [Hannoun et al. 1998]. These are due first to boundary layers existing along the tank bottom and side walls. Water in boundary layer travels at below-average velocities, residing in the compartments longer that τ. On the other hand, water away from the wall travels at above-average velocities, with shorter residence time. If combined with sudden expansions in flow area, boundary layers can separate from the wall, resulting in recirculation zones where flow reversal. To reduce the effect of boundary layer separation associated with flow expansions, baffle walls are commonly used, but they can also contribute to velocity gradients. In fact, since baffles force water around generally sharp turns, water particles on the outside of a turn must move faster that water on the inside. This gradient leads to different detention times and to stagnant water zones behind the turns. Finally, small inlets and outlets could produce velocity gradients since the velocity of water entering the tank through relatively small pipeline is significantly higher than the average velocity in the compartments [Hannoun et al. 1998]. The overall effect of the above flow disturbances is longitudinal mixing, which produces non-uniform residence times as well as microbial and chlorine concentration gradients [Greene 2002]. Hence, some part of the flow exits from the tank with less than the minimum amount of contact with the chlorine dose (short-circuiting), whereas other part of the flow has higher residence times due to dead zones existing in the tank. The ideal contact tank should be designed by reducing inlet and outlet velocities, distributing the water uniformly across the compartment cross-section, breaking up large scale eddies and preventing short-circuiting.

The paper presents the results of a Computational Fluid Dynamics (CFD) study undertaken to upgrading the performances of the contact tank of the wastewater treatment plant of Nola-Marigliano, near Napoli. Numerical simulations were performed to evaluate the hydraulic performances of the tank and to suggest some changes in its configuration in order to improve its performances.

2 THE APPLICATION OF CFD METHODS TO CONTACT TANKS

From the previous discussion it is evident how the disinfection effectiveness is strictly related to the contact tank hydraulic characteristics, that must be considered in details. Traditional approaches based on tracer studies and RTD models could

provide useful information about hydraulics of existing contact tanks only. Also, they are quite time consuming and expensive to perform on full-scale tanks and are unable to reveal all the factors controlling tank hydrodynamics. Hence, the application of CFD methods to simulate turbulent flow patterns within the tank, in conjunctions with disinfectant decay and microbial inactivation models, is becoming in recent years the best approach to contact tank design [Hannoun et al. 1998, Greene 2002, Wang et al. 2003]. Falconer and Liu [1987] have applied a 2D model to Elan contact tank comparing mean velocity distribution in the tank and flow through curves (FTC) predicted by the model with experimental data. Hannoun and Boulos [1997] and later Hannoun et al. [1998] applied a CFD model which predicts flow field and FTCs in order to improve existing contact tanks through the addiction of baffles. Other numerical studied were carried on in U.K on the Embsay contact tank, that has been experimentally investigated using a 1:8 scale model [Texiera and Shiono 1992, Shiono and Texeira 2000]. Modeled hydraulic characteristics and FTCs were compared with the experimental data [Falconer and Ismail 1997, Wang and Falconer 1998a, 1998b]. In some of these studies several combinations of different turbulent models and numerical schemes were tested against the measurements from a physical model of Embsay tank to identify the most suitable. Turbulent stresses were modeled using a depth mean eddy viscosity model and the k-ε model. Numerical results demonstrated that k-ε model gave a good prediction of horizontal recirculation in the tank compartments, but also it predicted a smaller cross-sectional average velocity toward the end of the tank. On the contrary, prediction from depth mean eddy viscosity model did not exhibit any recirculation region [Wang and Falconer 1998b]. Flow field and chlorine concentrations were modeled with good results in Elan contact tank using again different turbulent models and numerical schemes and comparing model prediction with experimental data [Wang et al., 2003]. Khan et al. [2006] carried out a 3D numerical simulation of the flow and the tracer transport inside the physical model used by Shiono and Texeira [2000] in their experiments using the standard k–ε model. Numerical data fairly reproduced the general mean velocity field and the FTC in contact tank, but the differences between computed velocities and data were generally higher in regions occupied by smaller eddies and involving some mixing. Gualtieri [2006] performed with the standard k–ε model steady-state and time-variable numerical simulations in a 2D geometry reproducing the physical model of Shiono and Texeira [2000]. Numerical results were in good agreements with the observed data for both flow and concentration field, especially in the compartments where experimental works have demonstrated that the flow could be considered as 2D. Then, RTD curve was derived for the tank and the numerical results were applied to evaluate the hydraulic efficiency of the tank using some literature performance indicators [Gualtieri and Pulci Doria 2007]. Rauen et al. [2008] compared new experimental results collected in a physical model of a contact tank with the numerical results from an improved low Reynolds number k–ε model to account for relatively low turbulence levels, similar to those occurring in the contact tank, particularly at the laboratory model scale. The comparison was successful, with the modified CFD code predicting the size of a typical mixing zone to within 90% accuracy and giving good agreement with the measured turbulence distribution. Texeira and Siqueira [2008] compared a number of hydraulic efficiency indicators widely applied in water and wastewater treatment units. They recommended the T_{10} as short-circuit indicator and the Morril Index MI as mixing indicator. This issue was also discussed by Gualtieri [2010]. Amini et al. [2011] applied the standard k–ε model to reproduce the 3D flow and tracer transport inside the 1:8 scaled-down physical model of Embsay chlorine contact tank. The simulations were validated against the experimental data from Shiono and Texeira [2000] and the effect of an increasing number of baffles on the extension of the recirculation regions behind the baffles and on the MI was investigated. Finally, a different baffles arrangement was suggested to further improve the hydraulic performance of the tank.

3 NUMERICAL SIMULATIONS

The flow inside a contact tank presents usually the feature that the variations of all

relevant quantities in the vertical direction, except in the thin boundary layer near channel bottom and possibly near the free surface, are substantially smaller that variations across the width or in streamwise direction. Hence, as a first approximation 2D or depth-averaged models may be applied. The simplest level of modeling a turbulent flow is the Reynolds Averaged Navier-Stokes (RANS) approach, where conservation laws for mass and momentum are averaged over a small time increment applying Reynolds decomposition, where flow quantities are decomposed in a temporal mean and a fluctuating component. Hence RANS equations are obtained, where the effect of turbulence appears as a number of terms representing the interaction between the fluctuating velocities and termed Reynolds stresses. They introduce closure problem, which can be solved, in analogy with the viscous stresses in laminar flow, by using an *eddy viscosity* [Kundu and Cohen 2004]. For a planar, incompressible flow RANS equations are:

$$\frac{\partial \overline{u}}{\partial x}+\frac{\partial \overline{v}}{\partial y}=0 \tag{2}$$

$$\begin{aligned}\overline{\rho}\left(\frac{\partial \overline{u}}{\partial t}+\overline{u}\,\frac{\partial \overline{u}}{\partial x}+\overline{v}\,\frac{\partial \overline{u}}{\partial y}\right)&=\overline{\rho}\,g_x-\frac{\partial \overline{p}}{\partial x}+\left(\mu+\rho\,v_t\right)\nabla^2\overline{u}\\ \overline{\rho}\left(\frac{\partial \overline{v}}{\partial t}+\overline{u}\,\frac{\partial \overline{v}}{\partial x}+\overline{v}\,\frac{\partial \overline{v}}{\partial y}\right)&=\overline{\rho}\,g_y-\frac{\partial \overline{p}}{\partial y}+\left(\mu+\rho\;v_t\right)\nabla^2\overline{v}\end{aligned} \tag{3}$$

where ρ and μ are fluid density and viscosity, p is fluid pressure and u, v are velocity components in the x and y directions, respectively. The overbar indicates time-averaged quantities. In the present study, for the closure problem, the standard k-ε model was applied. This model and its variation is the most widely used turbulence models and this is due to its ease in implementation, economy in computation and, most importantly, being able to obtain reasonable accurate solution with the available computer power. This model assumes an isotropic turbulence and the turbulent kinematic viscosity v_t in Eq. (3) could be estimated:

$$v_t=\frac{C_\mu\,k^2}{\varepsilon} \tag{4}$$

where k and ε are turbulent kinetic energy per mass unit and its dissipation rate, respectively, and C_μ=0.09. To estimate these parameters the two-equations of standard k-ε model are [Multiphysics 2009]:

$$\rho\frac{\partial k}{\partial t}+\rho\vec{\overline{V}}\cdot\nabla k=\nabla\cdot\left[\left(\frac{\mu+\mu_t}{\sigma_k}\right)\nabla k\right]+\frac{1}{2}\mu_t\left(\nabla\vec{\overline{V}}+\left(\nabla\vec{\overline{V}}\right)^T\right)^2-\rho\varepsilon \tag{5}$$

$$\rho\frac{\partial \varepsilon}{\partial t}+\rho\vec{\overline{V}}\cdot\nabla \varepsilon=\nabla\cdot\left[\left(\frac{\mu+\mu_t}{\sigma_\varepsilon}\right)\nabla \varepsilon\right]+\frac{1}{2}C_{1\varepsilon}\frac{\varepsilon}{k}\mu_t\left(\nabla\vec{\overline{V}}+\left(\nabla\vec{\overline{V}}\right)^T\right)^2-\rho C_{2\varepsilon}\frac{\varepsilon^2}{k} \tag{6}$$

where μ_t is dynamic eddy viscosity, whereas C_μ, σ_k, σ_ε, $C_{1\varepsilon}$ and $C_{2\varepsilon}$ are constants and their values are listed in Table 1.

Table 1. Values of the constants of the standard k-ε model

C_μ	σ_k	σ_ε	$C_{1\varepsilon}$	$C_{2\varepsilon}$
0.09	1.00	1.30	1.44	1.92

Transport of solutes in turbulent flow within the contact tank could be modelled using the 2D advection-diffusion equation for isotropic turbulence:

$$\frac{\partial \overline{C}}{\partial t}+\overline{u}\,\frac{\partial \overline{C}}{\partial x}+\overline{v}\,\frac{\partial \overline{C}}{\partial y}=\frac{\partial}{\partial x}\left(D_t\,\frac{\partial \overline{C}}{\partial x}\right)+\frac{\partial}{\partial y}\left(D_t\,\frac{\partial \overline{C}}{\partial y}\right) \tag{7}$$

where molecular diffusion was neglected and only turbulent diffusion was

considered with D_t as turbulent diffusivity and C as solute concentration.
The Eqs. from (2) to (7) were solved using Multiphysics 3.5a™ modeling package [Multiphysics 2009], providing the pressure, the velocity vector components, the k-ε model parameters and the solute concentration within the domain of the flow.

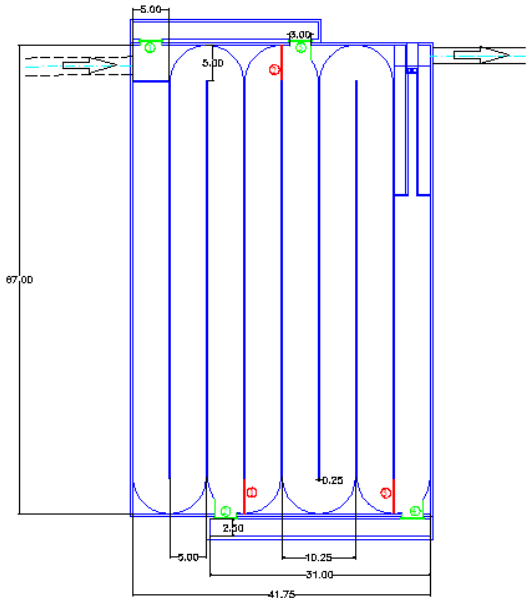

Figure 1. The contact tank of the Nola-Marigliano wastewater plant

Fig.1 shows the geometry of the contact tank with its dimensions (in meters). The tank is operating according two different schemes, namely A and B (Fig. 2). The flowrate entering the tank was 0.889 m³/s, resulting, for channel 5.0 m wide, in a mean water depth of 2.10 m and a mean cross-sectional velocity of 0.085 m/s. At the inlet, the velocity was of 0.217 m/s. Five simulations were carried out. Run A and B were performed to compare the hydraulic performances of A and B configurations. Later on, some different changes were proposed for configuration A, which has shown the best performances, to reduce dead-zones inside the tank and three other runs, namely Run C, D and E were done.
All the simulations were performed in two stages. First, steady-state turbulent flow within the tank was solved, using the k-ε model. Second, tracer transport was solved on top of this field flow in the time-domain by using Eq. (7), where the turbulent kinematic viscosity v_t was used as turbulent diffusivity. Tracer transport was analyzed in the case of a *burst* of concentration of a solute. For the simulations water with density ρ=999.05 kg/m³ and molecular viscosity μ=1.14·10⁻³ Kg/m×s, was selected as fluid. Boundary conditions were assigned at the inlet, the outlet, at the baffles and at the walls. For the k-ε model they were:

- at the inlet, an *inflow* type boundary condition was applied, with uniform velocity profile. Also inlet turbulent intensity and length scale were assigned. Turbulent intensity was set up to 5%, which corresponds to fully turbulent flows. The turbulent length scale was derived as 0.07×W, where W is the channel width;
- at the outlet, a *zero pressure* type condition was assigned;
- at walls and baffles, *logarithmic law of the wall* boundary condition was applied. To take into account of the walls effect on turbulent flow, an approach based on the so-called *wall functions* was applied to bridge the viscosity-affected region between the wall and the fully-turbulent region. Logarithmic wall functions applied to finite elements assume that the computational domain begins a distance δ_w from the real wall and the velocity can be described by:

$$u^+ = \frac{u}{u^*} = \frac{1}{\kappa} ln\left(\frac{\delta_W \, u^*}{v}\right) + C_1 \qquad (8)$$

where κ is Von Kármán constant, which is equal to 0.42, and C_1 is universal constant for smooth walls equal to 5.5 . The term in the round brackets is δ_w^+, that was assigned upon previous experiences equal to 100.

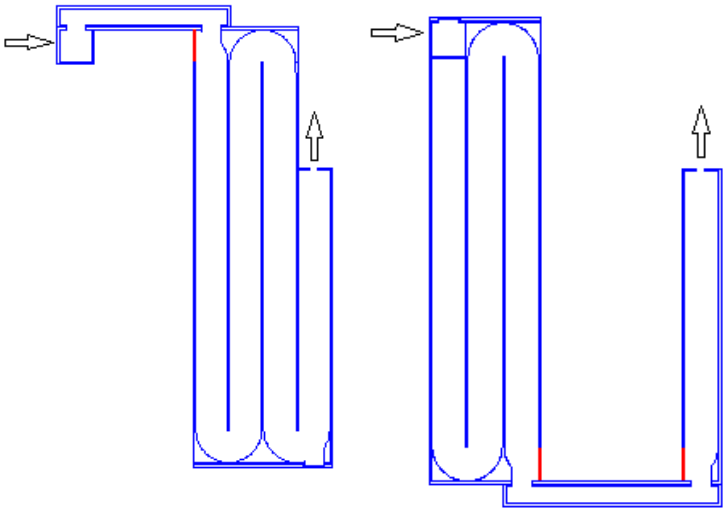

Figure 2. Operating schemes of the plant. Scheme A (left) and B (right).

For the advection-diffusion equation, boundary conditions were assigned at the inlet, the outlet, at the walls and in the injection point:

- at the inlet, to simulate the *burst* of concentration a time-dependent *concentration* boundary condition was applied with C_0=100 mol/m³:

$$C_{in}(t) = C_0 \, exp\left(-(t-2)^2\right) \tag{9}$$

- at the outlet, an *advective flux* type condition was assigned;
- at the baffles and at the walls, an *insulation* type condition was applied. This condition means that the solute cannot cross the walls;

The used mesh had a number of elements ranging from 38559 to 46172 with a minimum element quality of 0.798. Stationary segregated solver with non-linear system solver was used. For time-variable analysis, a time step of 10 seconds was selected extending the simulation until 6000 seconds. The concentration data were postprocessed to gain outlet tracer concentration, residence time distribution (RTD) function and the Morril Index:

$$MI = \frac{\theta_{90}}{\theta_{10}} \tag{10}$$

where θ_{10} and θ_{90} are the dimensionless time taken for the first 10% and 90% of flow entering to reach the outlet, respectively. *Mi* indicates the level of mixing in the tanks, since the higher is *MI* the higher is the level of mixing.

4 ANALYSIS OF RESULTS. DISCUSSION

Fig. 3 presents velocity field in the tank, with velocity values (the color of the tank surface) and velocity vectors (arrows). Higher velocities (red) were observed in horizontal by-pass channels and at the outlet, while low velocities (blue) were calculated in the corners and in the inner side of the compartments, where recirculation and flow reversal could be noted. These areas introduced dead-zones in the tank deviating flow patterns from ideal plug-flow conditions. These patterns were in agreement with those observed in the tank during its operation.

A comparison between Scheme A and B showed that the first was characterized by a lower percentage of dead zone and of the *M*I (Table 2). Hence, it was proposed to introduce some changes for Scheme A to improve its hydraulic performance.

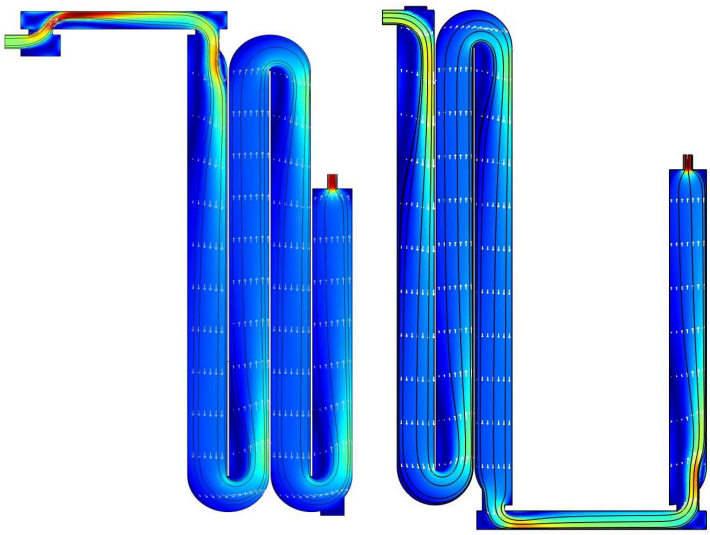

Figure 3. Velocity field for the Scheme A (left) and B (right).

In the Scheme C the inlet was from the by-pass channel, while in the Scheme D a grid of squared elements (0.1×0.1 m) with a center-to-center spacing 0.30 m, was added to each channel of the tank. Finally, in Scheme E, a grid of squared elements (0.25×0.25 m) with a center-to-center spacing 0.25 m, was inserted for 5.0 m into each baffle to reduce the dimensions of the dead-zones behind the baffles (Fig. 4). Only Scheme E produced a significant improvement of the hydraulic efficiency of the tank in terms of reduction of both dead-zones and MI (Table 2).

Table 2. Percentage of dead zones and *MI* for the considered operating schemes

Scheme	A	B	C	D	E
Dead zones − %	5.5	7.9	5.6	8.8	3.9
MI (θ_{90}/θ_{10})	1.454	1.506	1.438	1.769	1.375

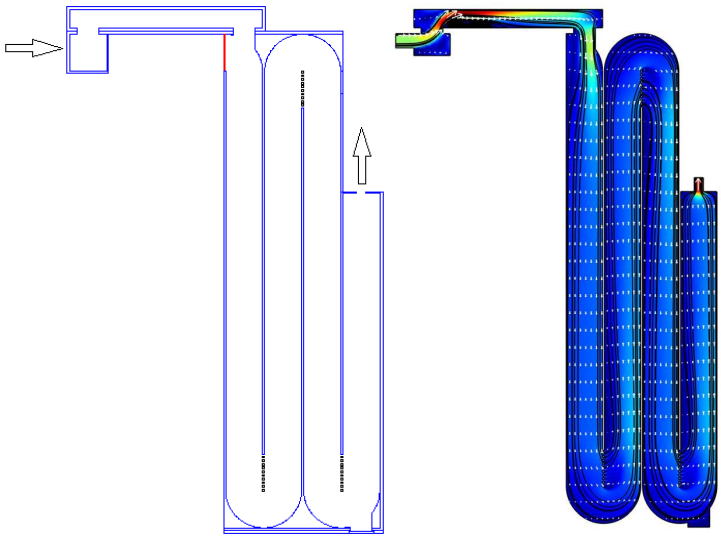

Figure 4. Scheme E (left) and velocity field for the Scheme E (right).

5 CONCLUSIONS

Understanding hydrodynamics and mass-transfer characteristics within a tank is

very useful in the design of this type of unit which are present both in water treatment plants and in water supply networks. The paper presented a numerical study carried out in the contact tank of the wastewater treatment plant of Nola-Marigliano (Napoli) to evaluate its hydraulic efficiency and to suggest some changes to the tank configuration to improve that. It was demonstrated that the introduction of a grid inside the baffles might allow a reduction of the dead-zones in the tank with a better approximation of the ideal plug-flow conditions. Overall, the study demonstrated that CFD methods could be applied to improve the hydraulic performances of existing contact tanks.

REFERENCES

Amini, R., Taghipour, R., and Mirgolbabaei, H., Numerical assessment of hydrodynamic characteristics in chlorine contact tank, *Int. J. Numer. Meth. Fluids,* 67**,** 885–898, 2011.

Falconer R.A. and Liu S.Q., Mathematical model study of plug flow in a chlorine contact tank, *Journal Water Environmental Management*, 1, 279–290, 1987.

Falconer R.A. and Ismail A.I.B.M., Numerical modelling of tracer transport in a contact tank, *Environmental International*, 23 (6), 763–773, 1997.

Greene D.J., Numerical simulation of chlorine disinfection process in non-ideal reactors, PhD Dissertation, Drexel University, U.S.A., 2002.

Gualtieri, C., Numerical simulations of flow and tracer transport in a disinfection contact tank. *iEMSs 2006*, Burlington, Vermont, USA, July 9/12, 2006.

Gualtieri, C., and Pulci Doria, G., Residence time distribution and dispersion in a contact tank. *XXXII IAHR Congress*, Venice, Italy, July 1/6, 2007.

Gualtieri, C., Discussion on E.C.Teixeira and R.N.Siqueira: Performance assessment of hydraulic efficiency indexes. J. Env.Eng., ASCE, 134 (10), 851−859. *J. Env. Eng., ASCE*, 136 (9), 1006−1007, 2010.

Gyurek L.L. and Finch G.R., Modeling water treatment chemical disinfection kinetics, *Journal of Environmental Engineering ASCE*, 124 (9), 783–793, 1998.

Hannoun I.A. and Boulos P.F., Optimizing distribution storage water quality: a hydrodynamic approach, *J. of Applied Mathematical Modeling*, 21, 495–502, 1997.

Hannoun I.A., Boulos P.F. and List E.J., Using hydraulic modelling to optimize contact time, *J. of American Water Works Assoc. (AWWA)*, August, 77–87, 1998.

Khan, L.A., Wicklein, E.A., and Teixeira, E.C., Validation of a three-dimensional computational fluid dynamics model of a contact tank, *J. Hydraul. Eng.*, 132 (7), 741–746, 2006.

Kundu, P.K., and Cohen, I.M., Fluid Mechanics, Elsevier Academic Prs, San Diego, CA, USA pp.760, 2004 (ISBN 978-0-12-178253-5).

Multiphysics 3.5a, User's Guide, ComSol AB, Sweden, 2009

Rauen, W.B., Lin, B., Falconer, R.A., and Teixeira. E.C., CFD and experimental model studies for water disinfection tanks with low Reynolds number flows, *Chemical Engineering Journal*, 137, 550–560, 2008.

Shiono K. and Texeira E.C., Turbulent characteristics in a baffled contact tank, *Journal of Hydraulic Research (JHR)*, 38 (6), 403–416, 2000.

Texeira E.C. and Shiono K., An investigation of the hydraulic behaviour of a chlorine contact tank, *Proceedings of 6th International Symposium on application of laser techniques to fluid mechanics and Workshop on computers in flow measurements*, Lisbon, Portugal, 1992.

Teixeira, E.C. and Siqueira, R.N., Performance assessment of hydraulic efficiency indexes. *J. Env.Eng*., ASCE, 134 (10), pp.851−859, 2008.

Wang H. and Falconer R.A., Simulating disinfection processes in chlorine contact tanks using various turbulence models and high-order accurate difference schemes, *Water Research*, 32 (5), 1529–1543, 1998a.

Wang H. and Falconer R.A., Numerical modelling of flow in chlorine disinfection tanks, *Journal of Hydraulic Engineering ASCE*, 124 (9), 918–931, 1998b.

Wang H., Shao X. and Falconer R.A., Flow and transport simulation models for prediction of chlorine contact tank flow-through curves, *Water Environment Research*, 75 (5), 455–471, 2003.